

ENHANCING CONTRAST AND RESOLUTION FOR ELECTRON-BEAM LITHOGRAPHY ON INSULATING SUBSTRATES

Deepak Kumar^{*}¹, Cooper Meyers¹, RJ Smith¹, and J. Todd Hastings^{†1,2}

¹Department of Electrical and Computer Engineering, University of Kentucky, Lexington, Kentucky 40506

²Department of Physics and Astronomy, University of Kentucky, Lexington, Kentucky 40506

May 7, 2025

ABSTRACT

We report on the effect of ambient gas on the contrast and the resolution of electron beam lithography (EBL) in gaseous environments on insulating substrates. Poly(methyl methacrylate) (PMMA) films were exposed in an environmental scanning electron microscope using a 30 keV electron-beam under 1 mbar pressure of helium, water, nitrogen and argon. We found that the choice of ambient gas results in significant variations in contrast, and the clearing dose increases with the gases' molecular weight and proton number, consistent with the increase in scattering cross-section. Significantly higher contrast values are obtained for exposure under helium and are accompanied by improved sensitivity. Despite higher sensitivity, helium exhibited the best resolution with 20-nm half-pitch dense lines and spaces. However, water vapor offered a larger process window, particularly on fused silica substrates. We also demonstrate that higher sensitivity results from effective charge dissipation. Thus, for EBL on insulating substrates, helium and water vapor may be desirable choices for charge dissipation depending on the substrate and process conditions.

Keywords electron beam lithography · nanofabrication · enhanced contrast · high-resolution · insulating substrates

1 Introduction

Lithography is the process of transferring patterns from one medium to another. Electron beam lithography (e-beam lithography or EBL) uses nanometer-sized focused electron beam for pattern transfer by irradiating substrates that have been coated with an organic or inorganic thin film resist that is sensitive to electrons. The solubility of the resist changes upon exposure to the electrons, allowing for selective removal of either the exposed region (positive-tone resist) or unexposed region (negative-tone resist) in a suitable developer solution. The pattern is finally transferred by either etching or lift-off.

The primary advantage of EBL over other lithographic techniques is that it provides (i) a maskless patterning process; (ii) high-resolution transfer of complex patterns with dimensions down to a few nanometers [Manfrinato et al. \[2019\]](#); and (iii) highly automated and precisely controlled operation. Because of its low throughput, EBL is primarily used in integrated-circuit photomask fabrication, small-volume production of semiconductor devices, and research [Pala and Karabiyik \[2012\]](#).

Some EBL applications require electrically insulating substrates including micromechanical systems, unconventional and organic semiconductor electronics, many photonic systems, and nanostructured optical elements. However, application of EBL for patterning on electrically insulating substrates is often limited because of surface charging effects. Considering the high beam energies employed (typically 30-100 kV) during EBL exposure process, much of the electron dose is deposited in the substrate. When the substrate is electrically insulating, the formation of strong electrostatic fields at the sample surface leads to charged-substrate electron-beam interaction causing the deflection of

^{*}deepak.kumar@uky.edu

[†]todd.hastings@uky.edu

the incident beam resulting in poor shape fidelity, pattern placement errors [Cummings and Kiersh \[1989\]](#), [Arat et al. \[2019\]](#), and even dielectric breakdown of the resist. Cumming et al. found that the charging problem was dependent on the beam current and independent of the dose, placing an upper limit on the beam current that can be used, hence limiting the write speed [Cumming et al. \[1997\]](#). Recently, pattern-placement error budgets for semiconductor mask writing have become limited by resist charging even on a nominally conductive EUV masks [Shamoun et al. \[2021\]](#). This problem has arisen because charge dissipation layers, such as those discussed below, introduce too many defects and reduce critical dimension control [Kim et al. \[2024\]](#).

Several methods have been developed to mitigate substrate charging while performing EBL on insulating substrates. Critical energy EBL (CE-EBL) [Joo et al. \[2006\]](#) takes advantage of the crossover energies between primary electron trapping and secondary electron emission to reduce pattern distortion. However, the resist thickness cannot be more than the penetration depth of the electron beam, and the crossover voltage depends on the substrate and the resist thickness as well as material properties. Owing to these limitations CB-EBL may not be the most practical option to reduce charging effects.

The most common method used for charge dissipation in EBL involves coating a thin conductive layer either on top or underneath the electron-beam resist. Conductive polymer coatings can be effective (see for example references [Angelopoulos et al. \[1993\]](#), [Huang \[1994\]](#), [Abargues et al. \[2008\]](#), [Dylewicz et al. \[2010\]](#)), but can be limited by a shorter shelf life and pH drift. Conductivity decreases when the pH moves outside the optimal range, increasing the risk of contamination upon precipitation of the polymers [Lopez et al. \[2019\]](#). As noted above, these are being abandoned for current generation EUV mask making.

Thin metal layers [Cumming et al. \[1997\]](#), [Samantaray and Hastings \[2008\]](#) are also effective for charge dissipation. Lower atomic number metal layer coatings have been found to significantly alter the clearing dose, but only slightly alter contrast and do not substantially degrade resolution [Samantaray and Hastings \[2008\]](#). Carbon films deposited by physical and chemical vapor deposition have also been considered for reducing resist charging on mask blanks. [Lin et al. \[2013\]](#) Film deposition prior to exposure and film removal prior to development can be time consuming, thus impacting the throughput. In addition, it is important to consider is the method used to deposit the metal layer. When compared to a thermally deposited aluminum layer, electron beam evaporation results in edge roughness that is more than three times higher and also increases the sensitivity of the resist to small dose variations [Hambitzer et al. \[2017\]](#). X-rays and electrons generated in the electron beam evaporator during deposition can also expose the resist [McCord and Michael \[1997\]](#).

Finally, variable-pressure electron-beam lithography (VP-EBL), which employs an ambient gas at subatmospheric pressures to reduce charging during EBL on electrically insulating substrates, has been found to be an efficient method for charge dissipation. Previous works demonstrated that low-pressure EBL can eliminate distortion and improve resolution when patterning PMMA on conducting [Paul \[1997\]](#) and insulating substrates [Myers and Dravid \[2006\]](#); there is a decrease in linewidth variability as chamber pressure increases. When using VP-EBL, there exists a trade-off between resist charging and decreasing linewidth dimensions [Paul \[1997\]](#). Recently it was shown that the introduction of water during the EBL exposure process, modifies the chemical processes during e-beam irradiation of Teflon AF [Sultan et al. \[2019\]](#) and also alters the sensitivity and contrast of PMMA on conductive substrate [Kumar et al. \[2023\]](#). However, no data is available on how the ambient gas affects the contrast of the process and the resolution of highly dense patterns on insulating substrates.

In this work, we studied the effect of ambient gas on the contrast and the resolution of highly dense patterns under various gases when patterning PMMA on insulating substrates. To our knowledge, these are the first studies of molecules other than water for EBL in gaseous environments. Choice of ambient gas results in significant variations in contrast. Clearing dose increases with the gases' molecular weight and proton number, consistent with the increase in scattering cross-section. High-resolution studies indicated that, despite higher sensitivity, helium exhibited the best resolution with 20-nm half-pitch dense lines and spaces. To our knowledge, this is the highest resolution demonstrated to date for EBL in a gaseous environment.

2 Experimental details

2.1 PMMA spin coating

PMMA (950 K molecular weight, MicroChem Corp.) was diluted using anisole (MicroChem Corp.) to make 4 wt. % and 1 wt. % solution for contrast and resolution experiments respectively. The PMMA solution thus prepared was spin coated onto a n-type (100) silicon, fused silica and soda lime glass substrate at 500 rpm for 5 s to give a uniform layer and then spun at 4000 rpm for 1 min to set the desired thickness. Next, the spin-coated substrates were heated on a hot plate at 180°C for 120 s to remove any residual solvent. Ellipsometry (M-2000, J. A. Woollam Co. Inc.) was used to

measure the final film thickness of the spin-coated PMMA film. The final resist thickness for the contrast and resolution experiments were measured to be 284 nm and 39 nm, respectively.

2.2 Variable-pressure electron-beam lithography process

An ELPHY Plus pattern generator (Raith GmbH) coupled with a FEI environmental scanning electron microscope (Quantum FEG 250) with a fast beam blanker was used for the VP-EBL process. A working distance of 10 mm and a beam energy of 30 keV were used for all lithographic processes. A Faraday cup and a pico-ammeter (Keithley 6487) were used for the beam current measurements under vacuum conditions prior to each lithographic exposure.

First, contrast curves were acquired for resist exposure under helium, water, nitrogen, and argon on fused silica and soda lime glass substrates. For contrast experiments, $20 \times 100 \mu\text{m}^2$ rectangular structures were exposed under 1 mbar pressure for each gas with areal exposure doses ranging from $10 - 300 \mu\text{C cm}^{-2}$ with a step size of 12.8 nm and a beam current of 89 pA. An electron-beam energy of 30 keV was chosen to reduce beam scattering in both gas and the resist, as well as to distribute backscattering to the largest range possible Newbury [2002]. Each adjacent rectangle was given a $20 \mu\text{m}$ spacing to minimize proximity effects from backscattering. To minimize any variations between exposures, patterns were placed on the same sample $400 \mu\text{m}$ apart from each other. Exposed films were developed in methyl isobutyl ketone and isopropyl alcohol (1:3 MiBK:IPA) for 60 s at room temperature followed by 30 s IPA rinse. The thicknesses of the resulting resist after development were measured using a Dektak 6M (Veeco, Inc.) surface profiler.

The second set of experiments was conducted to find the resolution limits for exposure under gaseous environment. For the resolution experiments, "nested-L" structures with 15, 20, 25, 50, 100 and 200 nm half-pitch were exposed under 1 mbar of ambient gases with line dose ranging from $50 - 700 \text{ pC cm}^{-1}$ in the increments of 50 pC cm^{-1} with a step size of 3.2 nm and a beam current of 68 pA. Each adjacent "nested-L" pattern was spaced by $4 \mu\text{m}$. The exposed film was developed in 4:1 ethanol:water for 45 s at 3°C followed by 10 s IPA rinse. Cold development of PMMA has been demonstrated to provide improved resolution with reduced line edge roughness Ocola and Stein [2006]. After exposure and development, the sample was sputter coated with 5 nm gold. An FEI environmental scanning electron microscope (Quantum FEG 250) and imageJ Schneider et al. [2012] were used for the line-width measurements.

3 Results and discussions

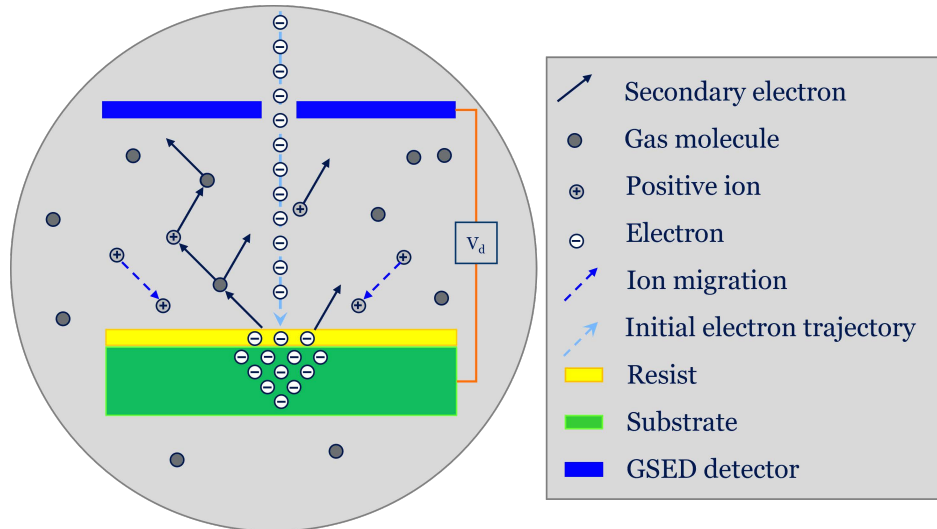


Figure 1: Schematic of VP-EBL. When performing EBL on insulating substrates, the bulk of the sample charges negatively by trapping primary electrons. Introducing a gas in the chamber can mitigate this charging process because the gas molecules may be ionized by electron impact. Typically multiple ions are generated through a cascade as secondary electrons are accelerated toward to the biased detector.

The use of VP-EBL to pattern under gaseous environment, shown in figure 1, involves the interactions of incident electrons with the gas and the subsequent formation of positive ions, mostly by secondary electrons, which affect the exposure process in several ways: (i) scattering of electrons in the gas could lead to a reduced effective absorbed dose in the resist, and (ii) incident primary electrons slow down under the applied detector voltage, resulting in a decreased

landing energy which affects the beam penetration, as well as the interaction volume, electron emission, and charging Stokes [2008]. Forward scattering in gas significantly affects the exposure process, Danilatos [1988] showed that the beam skirt radius from plural scattering in a gas is proportional to the effective atomic number of the scatterer; effective atomic number for helium, water, nitrogen, and argon are 2, 7.42, 7 and 18, respectively. For the conditions considered here, electron scattering in the gas results in an absorbed dose, D_{abs} , within the primary beam spot of

$$D_{abs_He} > D_{abs_N_2} > D_{abs_H_2O} > D_{abs_Ar} \quad (1)$$

During the VP-EBL exposure process, the secondary electrons emitted from the sample are accelerated toward a positively biased detector and multiplied as they ionize the ambient gas. The secondary electron cascade is collected by the detector and the resulting ions are accelerated toward the grounded or negatively charged substrate. The multiplication factor g , and thus the approximate number of ions per secondary electron generated Thiel [2004], is given by

$$g = e^{\alpha d} \quad (2)$$

where d is the detector-sample distance and α is the first Townsend ionization coefficient which is given by

$$\alpha = A \cdot P e^{-B \cdot P \cdot d \cdot V_0} \quad (3)$$

where A and B depend on the gas, V_0 is the applied detector voltage, and P is the pressure. P , V_0 and d were kept constant during our experiments; thus, the number of ions per secondary electron generated to balance surface charge is controlled by the choice of gas. In summary, electron scattering and ion generation in the ambient gas will alter the exposure process; electron scattering in gas reduces the absorbed dose, whilst ion amplification helps to minimize surface charge.

3.1 Effect of ambient gas on contrast and sensitivity

3.1.1 Sensitivity

Sensitivity, referred to here as the dose to clear or the clearing dose (D_C), is an inherent property of the resist and is defined as the minimum dose at which the exposed resist is soluble in the developer solution. Resist sensitivity depends on a large number of parameters, including resist material, resist thickness, developer, development time, and temperature, as well as the beam energy used for the exposure. There is a consistent trade-off between sensitivity and resolution for e-beam resists. Lower sensitivity is desirable when patterning is limited by shot noise. Ocola and Stein [2006] Higher sensitivity is desirable to increase throughput and/or minimize the required beam current Mkrtyan et al. [2000] as well as to reduce temperature rise in the resist Fares et al. [2000], Yasuda et al. [1994].

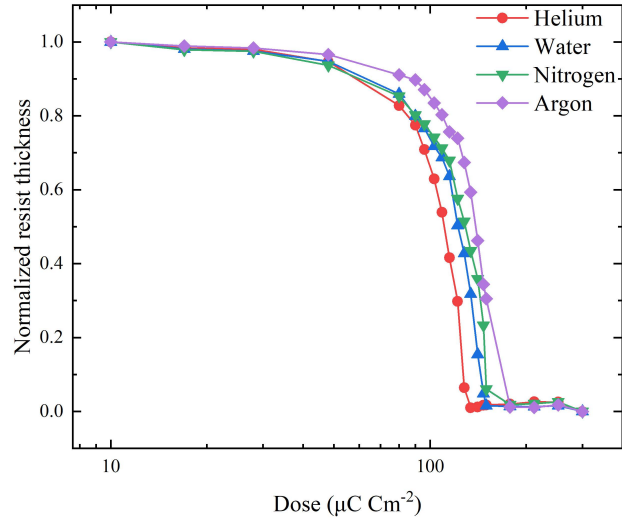
The sensitivity values of PMMA on soda lime glass and fused silica for exposure under different gases are tabulated in Table 1. The dose to clear, D_C , was obtained by fitting the data in to an empirical model described in detail in reference Ocola et al. [2015]. Soda lime glass differs from fused silica by the fact that it can be conductive at high fields due to the presence of mobile alkali ions Gedeon et al. [1999, 2000]. As previously stated, the sensitivity of resists on insulating substrates for exposure in a gaseous environment is influenced by electron scattering in gas and substrate charging. As is evident from Table 1, the dose to clear was found to increase with the gases' molecular weight and proton number, consistent with the increase in scattering cross-section. For the conditions that were investigated in this work, scattering was found to be the dominant contributor influencing the process's sensitivity. However, it is crucial to note that the influence of substrate charging is not inconsequential. When the sensitivity values for the two substrates for helium exposure are compared, the dose to clear is significantly reduced by 15% when using fused silica instead of soda lime glass.

3.1.2 Contrast

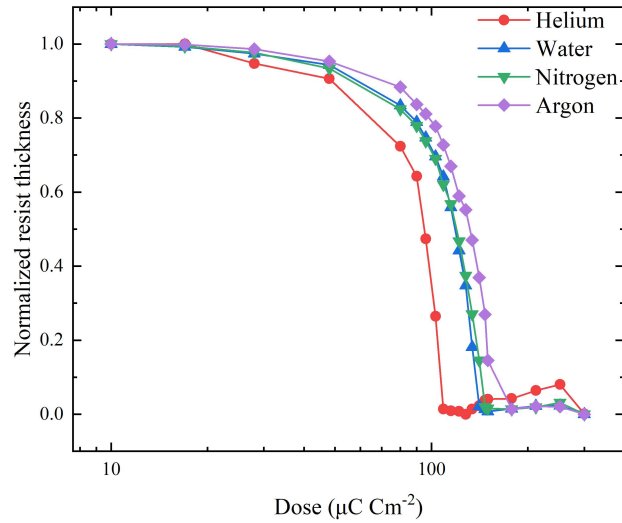
The resist contrast, which measures how non-linearly the development process responds to the chemical contrast created in the material after exposure, is crucial in determining the minimum image modulation that can be effectively transformed into a developed resist image Liddle et al. [2002]. Contrast describes how rapidly developed resist thickness changes with dose, which also has implications upon resolution. Combining contrast and sensitivity, the contrast curve of a resist can be obtained by plotting the residual resist thickness as a function of increasing electron dose. Higher contrast values result in steeper sidewall angles.

Table 1: Contrast (γ) and dose to clear (D_C) values of PMMA on soda lime glass and fused silica for exposure under ambient gases.

Chamber gas	Soda lime glass		Fused silica	
	D_C ($\mu\text{C cm}^{-2}$)	γ	D_C ($\mu\text{C cm}^{-2}$)	γ
Helium	130 ± 0	10.8 ± 0.4	110 ± 1	12.4 ± 0.9
Water	148 ± 0	9.4 ± 0.3	141 ± 0	9.9 ± 0.3
Nitrogen	158 ± 1	8.5 ± 0.3	145 ± 0	8.2 ± 0.2
Argon	160 ± 1	12.3 ± 0.5	158 ± 0	8.8 ± 0.2



(a) PMMA on soda lime glass



(b) PMMA on fused silica

Figure 2: Experimental data showing normalized resist thickness vs exposure dose for resist exposure under ambient gases of PMMA on (a) soda lime glass, and (b) fused silica.

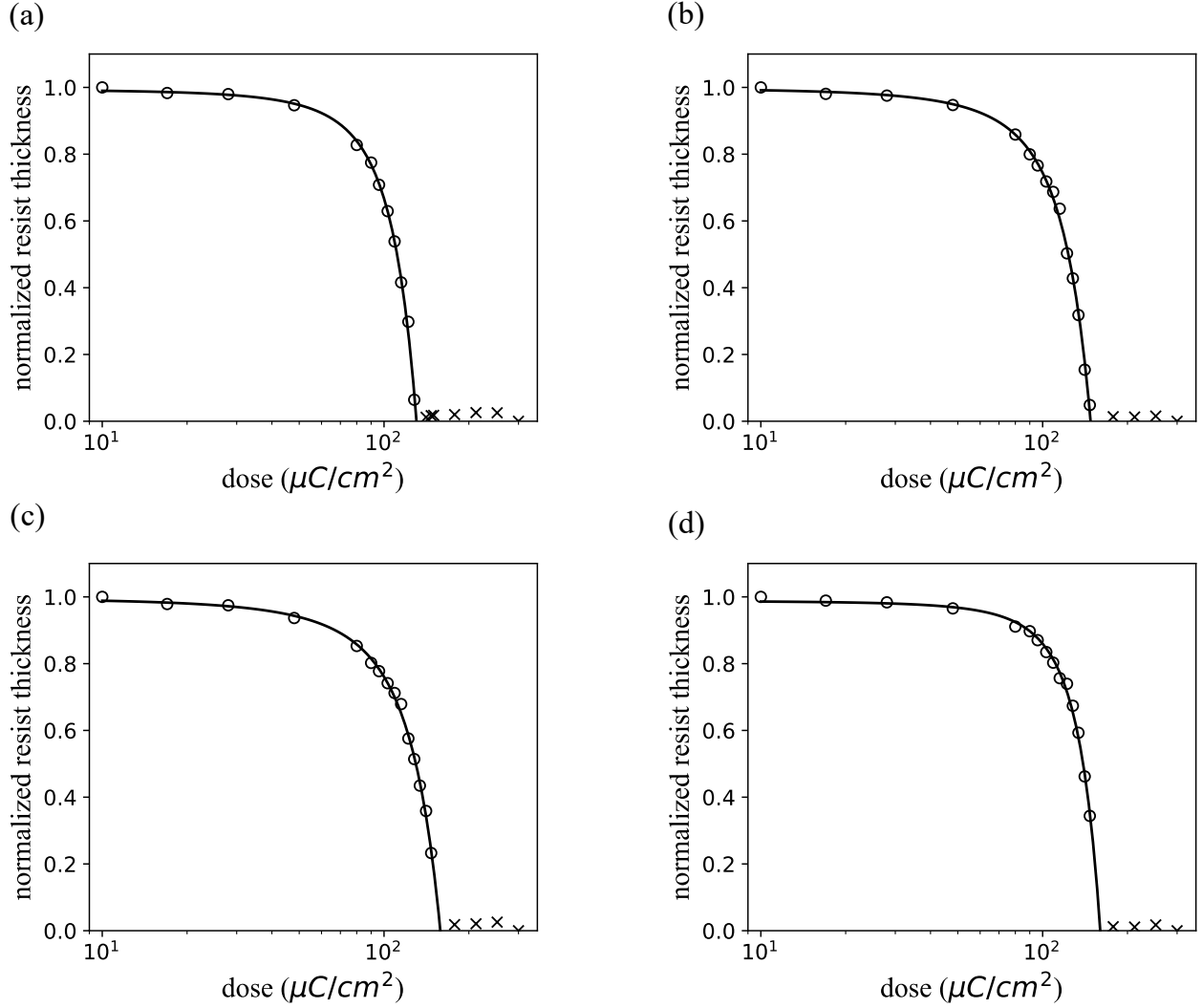


Figure 3: Fitted contrast curve (PMMA on soda lime glass) for exposure under 1 mbar of (a) Helium, (b) Water, (c) Nitrogen, and (d) Argon. Data points used for the fit are indicated by a \circ , while data points excluded from the fit are indicated by an \times .

The nature of the development process after the exposure determines the contrast value and is dependent on a number of elements including temperature, development time, developer solvents, and resist properties. Significant enhancement in contrast, at the cost of reduced sensitivity, is obtained for thick PMMA films developed at lower temperatures [Rooks et al. \[2002\]](#). However, for thin resist films, decreasing the development temperature does not have a discernible impact on contrast while reducing the sensitivity of PMMA to the developer [Hu et al. \[2004\]](#). The dose to clear is also greatly influenced by the choice of developer solvents and rinse solution. For PMMA, ethanol/ water in a 4:1 volume ratio offers a non-toxic alternative with superior contrast and resolution over current developers [Ocola et al. \[2015\]](#). Another method to improve resist contrast uses ultrasonically assisted development; the 3:7 water:IPA composition was found to be optimum for sensitivity and contrast [Yasin et al. \[2001\]](#). 200 keV EBL exposures lead to higher contrast than 30 keV exposures [Duan et al. \[2010\]](#). Contrast gradually increases with increasing water pressure at the expense of reduced sensitivity [Kumar et al. \[2023\]](#).

The contrast curves, normalized residual resist thickness versus areal exposure dose, of PMMA on soda lime glass and fused silica are plotted for different gases in Figure 2. Figures 3 and 4 illustrates the fitted contrast curves of PMMA on soda lime glass and fused silica. Data points used for the fit are indicated by a \circ , while data points excluded from the fit are indicated by an \times . Table 1 lists the contrast for exposure under different gases. Contrast, γ , was obtained by

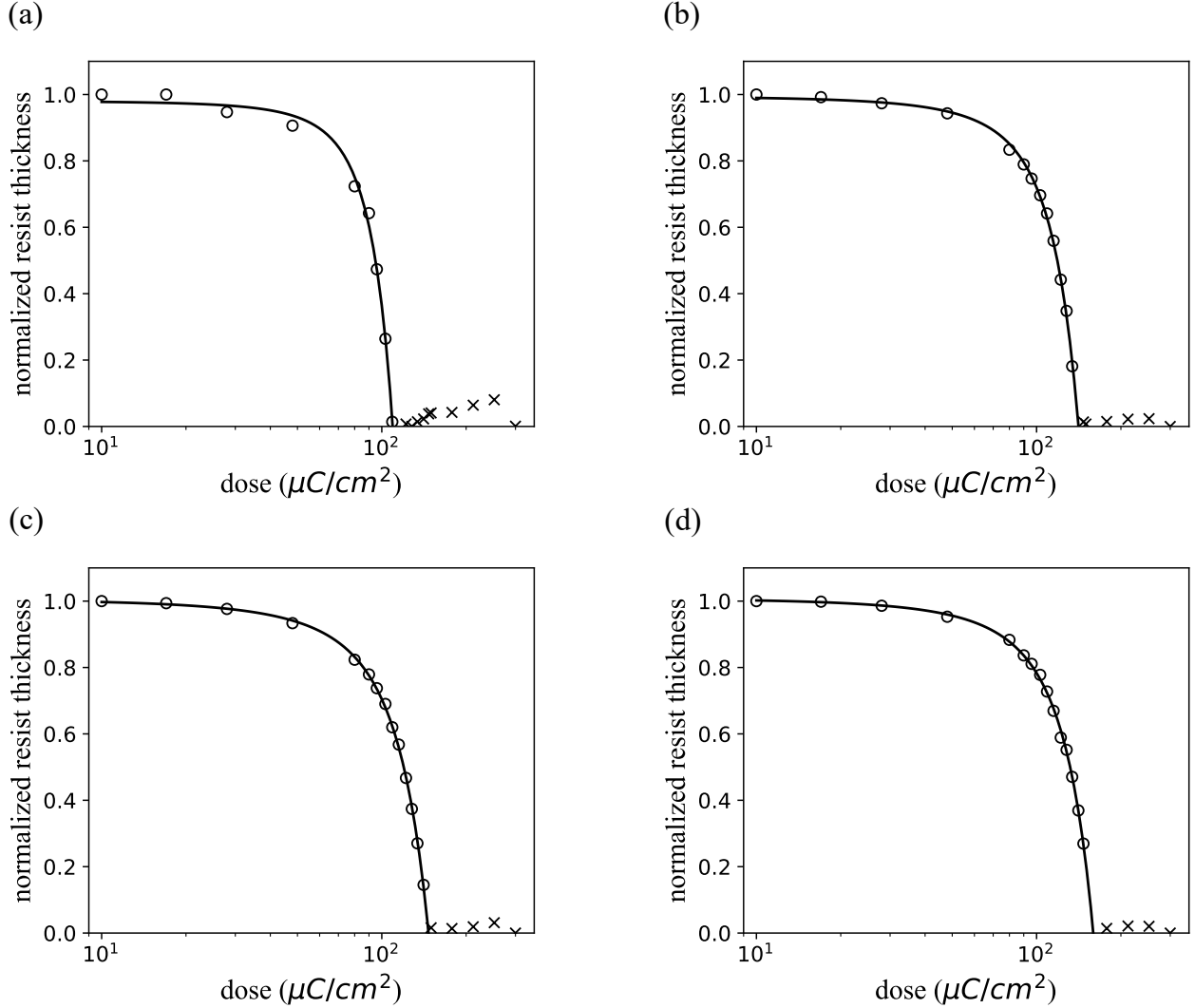


Figure 4: Fitted contrast curve (PMMA on fused silica) for exposure under 1 mbar of (a) Helium, (b) Water, (c) Nitrogen, and (d) Argon. Data points used for the fit are indicated by a \circ , while data points excluded from the fit are indicated by an \times .

fitting the data in to an empirical model described in detail in reference [Ocola et al. \[2015\]](#). Uncertainties represent the standard error of the fitted parameter.

Exposing PMMA on insulating substrates in a gaseous environment results in significant variations in contrast. Specifically, resist exposure under nitrogen or argon resulted in improved or degraded contrast values when compared to exposure under helium or water. Higher contrast is obtained for exposure under helium environment, which is also accompanied by substantially reduced dose to clear, which can be correlated to higher absorbed dose and effective charge dissipation. In order to better understand the physical mechanism that results in higher contrast and sensitivity for exposure under helium, we looked into how beam current influences the exposure process.

3.2 Effect of beam current on contrast and sensitivity

We examined the impact of the beam current on contrast and sensitivity to better understand the physical mechanism that leads to increased contrast and sensitivity. The beam current studies were restricted to fused silica substrates in order to remove any complexity related to the high field conductivity on soda lime glass substrates. It is evident from Table 2 that the process's sensitivity and contrast are not affected by the beam current when the exposure is carried out under water environment. However, there is a 12% decrease in the dose to clear at lower beam currents during exposure

Table 2: Contrast (γ) and dose to clear (D_C) of PMMA on fused silica for exposure at different beam currents.

Beam current	Water		Helium	
	D_C ($\mu\text{C cm}^{-2}$)	γ	D_C ($\mu\text{C cm}^{-2}$)	γ
78 pA	151 \pm 0	9.9 \pm 0.3	109 \pm 1	6.8 \pm 0.9
130 pA	151 \pm 0	10.1 \pm 0.3	112 \pm 1	6.6 \pm 0.4
191 pA	150 \pm 0	9.8 \pm 0.2	114 \pm 1	6.6 \pm 0.5
292 pA	149 \pm 0	9.6 \pm 0.3	123 \pm 1	7.6 \pm 0.5

Table 3: Contrast (γ) and dose to clear (D_C) of PMMA on soda lime glass and fused silica from loop exposures under water.

No. of loops	Soda lime glass		Fused silica	
	D_C ($\mu\text{C cm}^{-2}$)	γ	D_C ($\mu\text{C cm}^{-2}$)	γ
1	140 \pm 0	9.6 \pm 0.2	141 \pm 1	9.0 \pm 0.4
2	136 \pm 0	9.8 \pm 0.3	137 \pm 1	9.0 \pm 0.3
4	130 \pm 1	9.8 \pm 0.8	135 \pm 0	9.0 \pm 0.3
8	123 \pm 0	11.1 \pm 0.3	127 \pm 1	9.0 \pm 0.5

under helium environment, which can be correlated with effective charge dissipation. Lower beam currents result in higher sensitivity because the substrate has more time to discharge. It is also noteworthy that contrast drastically decreases with the number of exposures conducted under helium environment. This may be due to the resist being exposed by the helium ions. In order to examine the impact of refresh time, which gives the substrate additional time to discharge, we then carried out looped exposures.

3.3 Contrast and dose to clear from loop exposure experiments

The loop exposures were performed under water vapor to eliminate any possible exposure of the resist by helium ions. The fitted dose to clear values vs. the number of loops for PMMA on soda lime glass and fused silica is presented in Table 3. We see that the contrast does not change as the number of loops increases. A 10-12% reduction in dose to clear for 8 loop exposure is obtained, as would be expected when the substrate has more time to discharge. From these experiments, we conclude that effective charge dissipation tends to reduce the dose to clear.

3.4 High-resolution patterning on insulating substrates

Resolution defines the minimum feature size or the smallest distance between two patterns that can be resolved. Forward scattering of the beam in the resist and backscattering from the substrate adversely affect the resolution. Resolution is very closely related to both the sensitivity and contrast. It also becomes necessary to consider other factors including exposure charge density, beam accelerating voltage, resist thickness, and resist development process. Fabricating high-resolution sub-10 nm half-pitch features was found to be limited by the resist-development process [Duan et al. \[2010\]](#). Resist collapse upon development tends to limit resist film thicknesses to no more than three times the minimum feature size for a typical resist.

Fig. 5 compares high-resolution “nested-L” structures of PMMA on soda lime glass and fused silica for exposure under 1 mbar pressure of water vapor and helium. Exposure of PMMA on soda lime glass under both helium Fig. 5 (a) and water vapor Fig. 5 (b) exhibited the best resolution with 20-nm half-pitch dense lines and spaces clearly resolved. Exposure of PMMA on fused silica under water, Fig. 5 (d), exhibited the best resolution with 20-nm half-pitch. Despite higher sensitivity, exposure under helium (Fig. 5 (c)) can still exhibit the best resolution with 20-nm half-pitch at the cost of narrow process window. To the best of our knowledge, these are the highest resolution demonstrated to date for EBL in a gaseous environment.

3.5 Process window for high-resolution patterning

The process window for high-resolution patterning of PMMA on soda lime glass and fused silica for exposure under 1 mbar pressure of helium and water is compared in Fig. 6. The “✓” symbol here represent the clearly resolvable dense lines and spaces, “/” the underexposed or collapsed patterns, where as, “X” represent the unexposed or overexposed patterns. As can be seen, the process window is wider for exposure under water vapor on fused silica substrates,

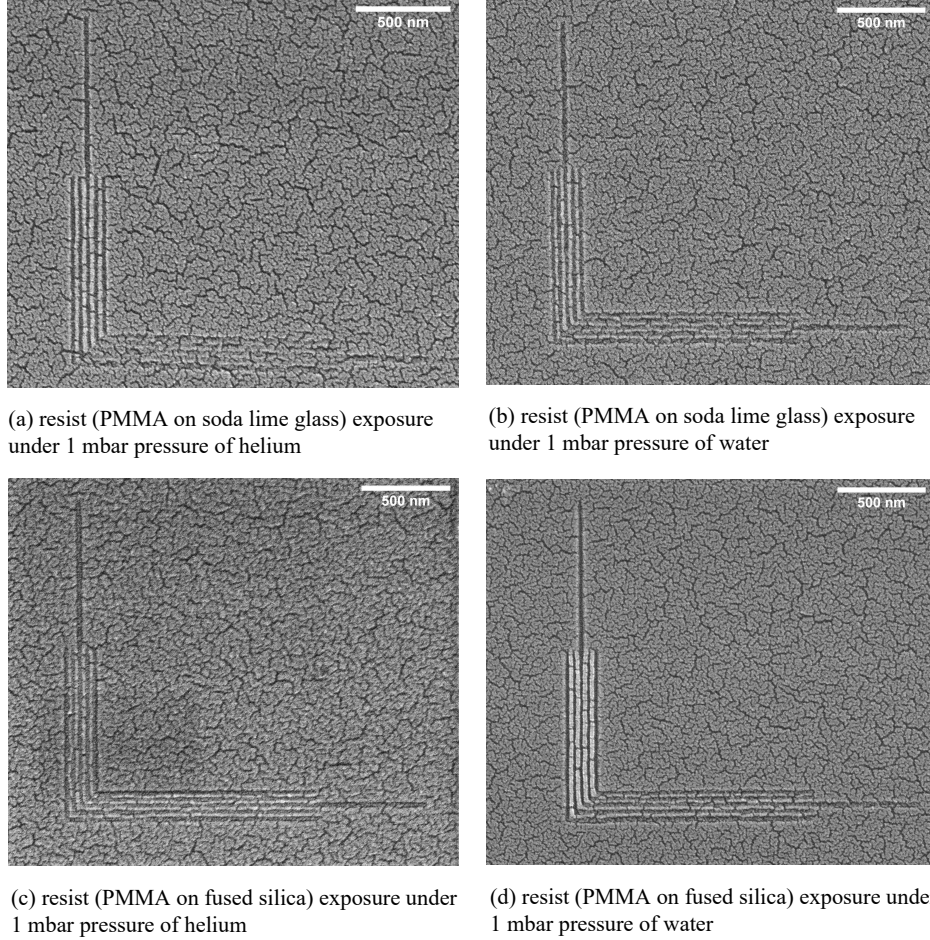


Figure 5: High resolution “nested-L” structures, 20 nm half-pitch; PMMA on soda lime glass exposed under (a) helium and (b) water; PMMA on fused silica exposed under (c) helium and (d) water.

whereas, the process window is wider for exposure under helium environment on soda lime glass substrates. Thus, for high-resolution patterning under gases, the choice of gas is substrate dependent.

4 Summary and conclusions

It was previously established that the introduction of water during electron beam lithography modifies the chemical processes during e-beam patterning of Teflon AF [Sultan et al. \[2019\]](#) and also alters the sensitivity and contrast of PMMA on conductive substrates [Kumar et al. \[2023\]](#). In this work, we studied the effect of ambient gas on the contrast and the resolution of dense patterns for EBL in gaseous environments when patterning PMMA on insulating substrates. To our knowledge, these are the first studies of molecules other than water for EBL in gaseous environments.

Clearing dose of PMMA was found to increase with the gases’ molecular weight and proton number, consistent with the increase in scattering cross-section. However, variation in contrast values were observed with different gases; especially, exposure under nitrogen and argon results in an improved or degraded contrast depending on the substrate. Regardless of the substrate, significantly higher contrast values are obtained for exposure under helium environment and are accompanied by an improvement in the sensitivity. In addition to the higher absorbed energy in the resist because of the less electron scattering in helium, possible exposure of the resist by helium ions may increase sensitivity. The contrast and dose to clear values for exposure on fused silica are found to improve by around 15% when comparing exposures on fused silica and soda lime glass in a helium environment.

Experiments studying the impact of beam current on contrast and sensitivity of PMMA on fused silica revealed that there is a 12% reduction in the dose to clear at lower beam currents during exposure under helium environment; however,

Half Pitch (nm)	Dose (pC cm ⁻¹)													
	50	100	150	200	250	300	350	400	450	500	550	600	650	700
Helium														
15	X	X	X	X	X	X	X	X	X	X	X	X	X	X
20	X	X	/	/	/	X	X	X	X	X	X	X	X	X
25	X	X	/	/	✓	✓	✓	✓	X	X	X	X	X	X
50	X	X	/	/	/	✓	✓	✓	✓	✓	✓	✓	✓	✓
100	X	X	/	/	✓	✓	✓	✓	✓	✓	✓	✓	✓	✓
200	X	X	/	/	✓	✓	✓	✓	✓	✓	✓	✓	✓	✓
Water														
15	X	X	X	X	X	X	X	X	X	X	X	X	X	X
20	X	X	X	X	/	X	X	X	X	X	X	X	X	X
25	X	X	X	X	X	/	✓	✓	X	X	X	X	X	X
50	X	X	X	X	/	/	/	✓	✓	✓	✓	✓	✓	✓
100	X	X	/	/	/	/	/	✓	✓	✓	✓	✓	✓	✓
200	X	X	/	/	/	/	/	✓	✓	✓	✓	✓	✓	✓

(a) PMMA on soda lime glass

Half Pitch (nm)	Dose (pC cm ⁻¹)													
	50	100	150	200	250	300	350	400	450	500	550	600	650	700
Helium														
15	X	X	X	X	X	X	X	X	X	X	X	X	X	X
20	X	X	/	X	X	X	X	X	X	X	X	X	X	X
25	X	X	✓	/	X	X	X	X	X	X	X	X	X	X
50	X	X	/	✓	✓	✓	✓	X	X	X	X	X	X	X
100	X	/	✓	✓	✓	✓	✓	X	X	X	X	X	X	X
200	X	/	✓	✓	✓	✓	✓	X	X	X	X	X	X	X
Water														
15	X	X	/	/	/	X	X	X	X	X	X	X	X	X
20	X	X	X	/	/	✓	/	/	X	X	X	X	X	X
25	X	X	X	/	✓	✓	✓	✓	✓	/	/	/	X	X
50	X	X	/	/	✓	✓	✓	✓	✓	✓	✓	✓	✓	✓
100	X	X	X	/	/	✓	✓	✓	✓	✓	✓	✓	✓	✓
200	X	X	X	/	/	✓	✓	✓	✓	✓	✓	✓	✓	✓

(b) PMMA on fused silica

Figure 6: Process window for high-resolution patterning for exposure under helium and water for PMMA on (a) soda lime glass and (b) fused silica. "X" indicates unresolved patterns, "/" indicates underdeveloped or collapsed patterns, and "✓" indicates fully resolved patterns.

contrast drastically decreases with the number of exposures. The improvement in sensitivity and reduction in contrast is correlated to effective charge dissipation and the resist being exposed by helium ions. These are corroborated from results obtained from looped exposures. A reduction of 10-12% in the dose to clear is obtained with increasing the number of exposure loops. From these results, we conclude that effective charge dissipation tends to reduce the dose to clear.

High-resolution patterning studies indicated that despite higher sensitivity helium still exhibited the best resolution (20-nm half-pitch lines and spaces) but at the cost of a narrow process window. This appears to be the highest resolution demonstrated to date for EBL in gaseous environments. The process window for high-resolution patterning on insulating substrates in a gaseous environment is substrate dependent. On fused silica substrates, the process window is wider when exposed under water; on soda lime glass substrates, it is wider when exposed under helium. Thus, on insulating substrates for EBL in gaseous environment, helium yields higher sensitivity without sacrificing resolution.

5 Acknowledgments

This work was supported by the National Science Foundation (NSF) under Grant No. CMMI-2135666. This work was performed, in part, at the University of Kentucky Center for Nanoscale Science and Engineering and Electron Microscopy Center, members of the National Nanotechnology Coordinated Infrastructure (NNCI), which was supported by the National Science Foundation (No. NNCI-2025075).

References

- Vitor R Manfrinato, Fernando E Camino, Aaron Stein, Lihua Zhang, Ming Lu, Eric A Stach, and Charles T Black. Patterning si at the 1 nm length scale with aberration-corrected electron-beam lithography: tuning of plasmonic properties by design. *Advanced Functional Materials*, 29(52):1903429, 2019.
- Nezih Pala and Mustafa Karabiyik. Encyclopedia of nanotechnology, chapter electron beam lithography (ebl), 2012.
- KD Cummings and M Kiersh. Charging effects from electron beam lithography. *Journal of Vacuum Science & Technology B: Microelectronics Processing and Phenomena*, 7(6):1536–1539, 1989.
- Kerim T Arat, Thomas Klimpel, Aernout C Zonneville, Wilhelmus SMM Ketelaars, Carel Th H Heerkens, and Cornelis W Hagen. Charge-induced pattern displacement in e-beam lithography. *Journal of Vacuum Science & Technology B*, 37(5), 2019.
- David RS Cumming, Iman I Khandaker, Stephen Thoms, and Brendan G Casey. Efficient diffractive optics made by single-step electron beam lithography in solid pmma. *Journal of Vacuum Science & Technology B: Microelectronics and Nanometer Structures Processing, Measurement, and Phenomena*, 15(6):2859–2863, 1997.
- Bassam Shamoun, Mahesh Chandramouli, Bin Liu, Reid K Juday, Igal Bucay, Andrew T Sowers, and Frank E Abboud. Multi-beam mask writer in euv era: challenges and opportunities. *Novel Patterning Technologies 2021*, 11610:64–82, 2021.
- Hyoyeon Kim, Hyungrae Noh, Wonsik Shin, Kangho Park, Youngjae Lee, Sangho Jo, Youngsu Sung, Hojune Lee, Heebom Kim, Jin Choi, et al. Improvement of mask pattern placement error using novel resist charging control methodology in multi-beam mask writer. In *Photomask Japan 2024: XXX Symposium on Photomask and Next-Generation Lithography Mask Technology*, volume 13177, pages 266–279. SPIE, 2024.
- Jaebum Joo, Brian Y Chow, and Joseph M Jacobson. Nanoscale patterning on insulating substrates by critical energy electron beam lithography. *Nano letters*, 6(9):2021–2025, 2006.
- Marie Angelopoulos, Niranjana Patel, Jane M Shaw, Nancy C Labianca, and Stephen A Rishton. Water soluble conducting polyanilines: applications in lithography. *Journal of Vacuum Science & Technology B: Microelectronics and Nanometer Structures Processing, Measurement, and Phenomena*, 11(6):2794–2797, 1993.
- Wu-Song Huang. Synthesizing and processing conducting polythiophene derivatives for charge dissipation in electron-beam lithography. *Polymer*, 35(19):4057–4064, 1994.
- R Abargues, U Nickel, and PJ Rodriguez-Canto. Charge dissipation in e-beam lithography with novolak-based conducting polymer films. *Nanotechnology*, 19(12):125302, 2008.
- R Dylewicz, S Lis, RM De La Rue, and F Rahman. Charge dissipation layer based on conductive polymer for electron-beam patterning of bulk zinc oxide. *Electronics letters*, 46(14):1025–1027, 2010.
- Gerald Lopez, Glen de Villafranca, Grant Shao, Meiyue Zhang, and Andrew Thompson. Charge dissipation by use of a novel aqueous based quaternary ammonium compound for use in electron beam lithography on non-conductive substrates. In *Advances in Patterning Materials and Processes XXXVI*, volume 10960, pages 283–290. SPIE, 2019.
- CB Samantaray and JT Hastings. The effect of thin metal overlayers on the electron beam exposure of polymethyl methacrylate. *Journal of Vacuum Science & Technology B: Microelectronics and Nanometer Structures Processing, Measurement, and Phenomena*, 26(6):2300–2305, 2008.
- Yun-Yue Lin, Hsin-Chang Lee, Chia-Jen Chen, Ta-Cheng Lien, and Anthony Yen. Method of making a lithography mask, October 2013. US Patent App. 13/437,565.
- Anna Hambitzer, Antonis Olziersky, Tamara Saranovac, and Colombo R Bolognesi. Comparison of charge dissipation layers and dose sensitivity of pmma electron beam lithography on transparent insulating substrates such as gan. In *International Conference on Compound Semiconductor Manufacturing Technology (CS ManTech 2017)*, Indian Wells, CA, US, 2017.
- MA McCord and RJ Michael. Electron beam lithography, handbook of microlithography, micromachining and microfabrication, vol. 1, 1997.

- BK Paul. Effects of gas pressure on low-pressure electron-beam lithography. *Scanning*, 19(7):466–468, 1997.
- Benjamin D Myers and Vinayak P Dravid. Variable pressure electron beam lithography (vp-e bl): A new tool for direct patterning of nanometer-scale features on substrates with low electrical conductivity. *Nano letters*, 6(5):963–968, 2006.
- Mansoor A Sultan, Sarah K Lami, Armin Ansary, Douglas R Strachan, Joseph W Brill, and J Todd Hastings. Altering the radiation chemistry of electron-beam lithography with a reactive gas: a study of teflon af patterning under water vapor. *Nanotechnology*, 30(30):305301, 2019.
- Deepak Kumar, Krishnaroop Chaudhuri, Joseph W Brill, Jonathan T Pham, and J Todd Hastings. Effect of water vapor pressure on positive and negative tone electron-beam patterning of poly (methyl methacrylate). *Journal of Vacuum Science & Technology B*, 41(1), 2023.
- Dale E Newbury. X-ray microanalysis in the variable pressure (environmental) scanning electron microscope. *Journal of Research of the National Institute of Standards and Technology*, 107(6):567, 2002.
- LE Ocola and A Stein. Effect of cold development on improvement in electron-beam nanopatterning resolution and line roughness. *Journal of Vacuum Science & Technology B: Microelectronics and Nanometer Structures Processing, Measurement, and Phenomena*, 24(6):3061–3065, 2006.
- Caroline A Schneider, Wayne S Rasband, and Kevin W Eliceiri. Nih image to imagej: 25 years of image analysis. *Nature methods*, 9(7):671–675, 2012.
- Debbie Stokes. *Principles and practice of variable pressure/environmental scanning electron microscopy (VP-ESEM)*. John Wiley & Sons, 2008.
- GD Danilatos. Foundations of environmental scanning electron microscopy. In *Advances in electronics and electron physics*, volume 71, pages 109–250. Elsevier, 1988.
- Bradley L Thiel. Master curves for gas amplification in low vacuum and environmental scanning electron microscopy. *Ultramicroscopy*, 99(1):35–47, 2004.
- M Mkrtchyan, E Munro, JA Liddle, ST Stanton, WK Waskiewicz, RC Farrow, and V Katsap. Global space charge effect in scalpel. *Microelectronic engineering*, 53(1-4):299–302, 2000.
- N Fares, S Stanton, J Liddle, and G Gallatin. Analytical-based solutions for scalpel wafer heating. *Journal of Vacuum Science & Technology B: Microelectronics and Nanometer Structures Processing, Measurement, and Phenomena*, 18(6):3115–3121, 2000.
- M Yasuda, H Kawata, K Murata, K Hashimoto, Y Hirai, and N Nomura. Resist heating effect in electron beam lithography. *Journal of Vacuum Science & Technology B: Microelectronics and Nanometer Structures Processing, Measurement, and Phenomena*, 12(3):1362–1366, 1994.
- Leonidas E Ocola, Maya Costales, and David J Gosztola. Development characteristics of polymethyl methacrylate in alcohol/water mixtures: a lithography and raman spectroscopy study. *Nanotechnology*, 27(3):035302, 2015.
- Ondrej Gedeon, Karel Jurek, and Václav Hulínský. Fast migration of alkali ions in glass irradiated by electrons. *Journal of non-crystalline solids*, 246(1-2):1–8, 1999.
- Ondrej Gedeon, Václav Hulínský, and Karel Jurek. Microanalysis of glass containing alkali ions. *Microchimica Acta*, 132:505–510, 2000.
- J Alexander Liddle, Gregg M Gallatin, and Leonidas E Ocola. Resist requirements and limitations for nanoscale electron-beam patterning. *MRS Online Proceedings Library (OPL)*, 739:H1–5, 2002.
- MJ Rooks, E Kratschmer, R Viswanathan, J Katine, RE Fontana Jr, and SA MacDonald. Low stress development of poly (methylmethacrylate) for high aspect ratio structures. *Journal of Vacuum Science & Technology B: Microelectronics and Nanometer Structures Processing, Measurement, and Phenomena*, 20(6):2937–2941, 2002.
- Wenchuang Hu, Koshala Sarveswaran, Marya Lieberman, and Gary H Bernstein. Sub-10 nm electron beam lithography using cold development of poly (methylmethacrylate). *Journal of Vacuum Science & Technology B: Microelectronics and Nanometer Structures Processing, Measurement, and Phenomena*, 22(4):1711–1716, 2004.
- Shazia Yasin, DG Hasko, and H Ahmed. Fabrication of < 5 nm width lines in poly (methylmethacrylate) resist using a water: isopropyl alcohol developer and ultrasonically-assisted development. *Applied Physics Letters*, 78(18):2760–2762, 2001.
- Huigao Duan, Donald Winston, Joel KW Yang, Bryan M Cord, Vitor R Manfrinato, and Karl K Berggren. Sub-10-nm half-pitch electron-beam lithography by using poly (methyl methacrylate) as a negative resist. *Journal of Vacuum Science & Technology B*, 28(6):C6C58–C6C62, 2010.